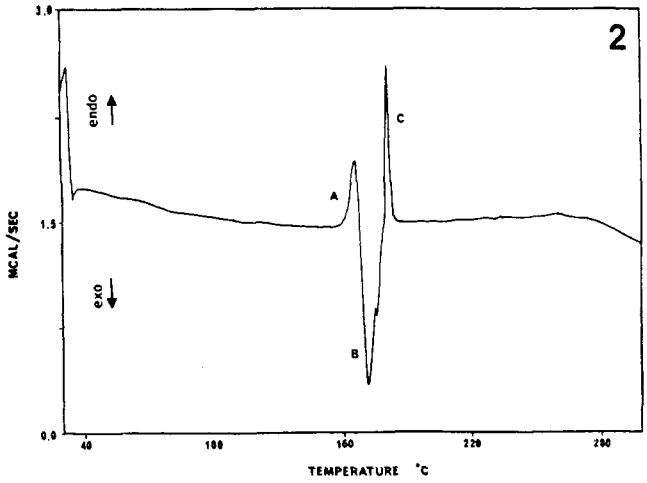

Figure 2. Differential scanning calorimetry curve for *trans*-$RuCl_2(CO)(PhMe_2P)_3$. The heating rate is 20 °C/min under nitrogen. The number in the upper right corner refers to the compound number given in Table I.

Like the trans complexes **2** and **3**, the *ttt* complex **4** undergoes a slight amount of melting before isomerization to the *cct* isomer. The isomerized product melts at 223 °C, about 5 °C lower than that of the pure *cct* isomer (228–230 °C).

The DSC curve for complex **5** shows a much more pronounced endotherm than the previous complexes. Not surprisingly, visual observations show that the *ttt* complex melts entirely before isomerization. No endotherm is seen for the melting of the *cct* isomer, because the *cct* isomer actually melts at a lower temperature than the *ttt* isomer (134–135 vs 143 °C).

For complex **6**, *ttt*-$RuCl_2(CO)_2(Me_3P)_2$, complete melting of the *ttt* isomer occurs before isomerization. However, two exotherms are evident in the DSC curve. The first appears to be the result of the *ttt* to *cct* isomerization in the liquid state. Because the melting point of the *cct* isomer is 196–198 °C, the following exotherm is probably due to the fusion *cct* (liquid) → *cct* (solid). A sharp endotherm observed at 200 °C corresponds to the melting of the *cct* isomer.

The isomerization of complex **7** also occurs in the solid state. An exotherm at 158 °C is well separated from the melting of the *cct* isomer at 228 °C. This correlates well with what was observed for the melting point of the *cct* isomer (227–229 °C).

The final complex investigated was *ccc*-$RuCl_2(CO)_2(Ph_2MeP)_2$ (**8**). An exotherm that commences at 138 °C in its DSC curve seems to indicate a solid-state isomerization. When the complex is viewed in a melting point capillary, a color change to dark orange occurred in this temperature region. Considerable compression of the sample occurred, but the sample appeared to remain solid. At 220 °C the orange product melted, which is close to the melting point of the *cct* isomer (228 °C).

The visual observations and DSC results described above seem to indicate that complexes **1**, **4**, **7**, and **8** isomerize in the solid state. For **2** and **3** isomerization commenced in the solid state but melting ensued before isomerization was complete. That the cis (or *cct*) isomer is the product in all cases was verified by ^{31}P NMR spectroscopy.[1] Solid samples of **2–6** and **8** were placed in 10-mm NMR tubes and heated in an oven at 190 °C for 55 min. After the samples were cooled to room temperature, $CDCl_3$ was added to each tube and the NMR spectrum recorded. Each spectrum showed the cis or *cct* isomer to account for greater than 90% of the phosphorus in the sample.

Measurements of the areas under the endotherms and exotherms of the DSC curves allow one to estimate the enthalpy of fusion, ΔH_f, and the enthalpy of isomerization, ΔH_i. The values for the heat of fusion for the trans isomers **2** and **3** are likely to be too low due to the incomplete melting of these complexes. The value for the heat of isomerization for complex **6** may be too high because of the overlapping fusion exotherm.

Certain conclusions can be drawn from the DSC results collected in Table I. First, the temperature at which isomerization occurs is largely independent of the number or identity of the phosphines. All of the complexes appear to isomerize between 140 and 180 °C in the solid state. The enthalpy of isomerization also shows no clear trend based on the phosphine ligand, although for the $(R_3P)_3Ru(CO)Cl_2$ complexes the isomerization enthalpy decreases with increasing steric bulk of the phosphine. Heats of fusion are generally lower for the cis complexes (or *cct* complexes) than for the trans complexes. This is in agreement with what has been found by Kukushkin et al., for a series of platinum complexes[9] of the type *cis*- and *trans*-$PtCl_2(PhNH_2)$(triethyl phosphate).

Although we have made no attempt to investigate the kinetics of these solid-state isomerizations, a qualitative ordering of the relative rates can be obtained by comparing the shapes of the isomerization exotherms for DSC curves obtained at the same heating rate. The rates of isomerization appear to decrease in the order **2** > **4**, **5** > **6** > **3** > **1** > **8**. This ordering is not the same as found for these same complexes in solution.

As an additional consideration, the solid-state isomerizations of these complexes may be useful as a means of preparing the thermodynamically preferred isomers. The ^{31}P NMR data have confirmed that the cis or *cct* isomers are formed in very good yield by this method. In solution thermal isomerization[1] of *ttt*-$(R_3P)_2Ru(CO)_2Cl_2$ may lead to mixtures of *ccc*-$(R_3P)_2Ru(CO)_2Cl_2$, *cct*-$(R_3P)_2Ru(CO)_2Cl_2$, $[(R_3P)_2Ru(CO)Cl_2]_2$, and *trans*-$(R_3P)_3Ru(CO)Cl_2$.

Acknowledgment is made to the donors of the Petroleum Research Fund, administered by the American Chemical Society, for financial support.

Supplementary Material Available: Differential scanning calorimetry curves for compounds **3–8** (6 pages). Ordering information is given on any current masthead page.

(9) Kukushkin, Y. N.; Budanova, V. F.; Sedova, G. N. *Zh. Neorg. Khim.* **1976**, *21*, 1405; *Russ. J. Inorg. Chem. (Engl. Transl.)* **1976**, *21*, 768.

Contribution from the Department of Chemistry, University of California, Davis, California 95616

Synthesis and Structure of a Heterometallic Cluster with a Novel Layered Structure: $[W(CO)_5SnClFe(CO)_4]_2[Na_2((C_2H_5)_2O)_4(C_4H_8O_2)]$

Alan L. Balch,* Marilyn M. Olmstead, and Douglas P. Oram

Received April 21, 1988

Recently, considerable attention has been focused on transition-metal complexes with "naked" main-group ligands.[1,2] Continuing our own work on main group–transition metal interactions[3,4] which has added examples of one- and two-coordinate thallium[5,6] to these, we attempted to create an example of a substituent-free complex derived from Sn(II). Thus, we examined the reaction between $(OC)_5WSnCl_2$(tetrahydrofuran)[4] and $Fe(CO)_4^{-2}$ expecting to form the hypothetical "$(OC)_5WSn{=}Fe$-

(1) Herrmann, W. A. *Angew. Chem., Int. Ed. Engl.* **1986**, *25*, *56* and references therein.
(2) Huttner, G.; Weber, U.; Sigwarth, B.; Scheidsteger, O.; Lang, H.; Zsolnai, L. *J. Organomet. Chem.* **1985**, *282*, 331 and references therein.
(3) Olmstead, M. M.; Benner, L. S.; Hope, H.; Balch, A. L. *Inorg. Chim. Acta* **1979**, *32*, 193. Blach, A. L.; Hope, H.; Wood, F. E. *J. Am. Chem. Soc.* **1985**, *107*, 6936.
(4) Balch, A. L.; Oram, D. E. *Organometallics*, **1988**, *7*, 155.
(5) Balch, A. L.; Nagle, J. K.; Olmstead, M. M.; Reedy, P. E., Jr. *J. Am. Chem. Soc.* **1987**, *109*, 4123.
(6) Nagle, J. K.; Balch, A. L.; Olmstead, M. M. *J. Am. Chem. Soc.* **1988**, *110*, 319.

0020-1669/88/1327-4309$01.50/0

Table I. Atomic Coordinates ($\times 10^4$) and Isotropic Thermal Parameters ($Å^2 \times 10^3$) for **1**

	x	y	z	U
Fe	−1537 (1)	−915 (1)	653 (1)	22 (1)[a]
W	1216 (1)	−1059 (1)	3332 (1)	26 (1)[a]
Sn	78 (1)	23 (1)	1289 (1)	20 (1)[a]
Cl	−1680 (3)	1872 (2)	1546 (2)	38 (1)[a]
Na	−3326 (4)	3363 (3)	2627 (3)	29 (1)[a]
C(1)	1021 (13)	−2618 (11)	3441 (10)	43 (3)
C(2)	3203 (12)	−1275 (10)	2497 (9)	40 (2)
C(3)	1221 (11)	583 (10)	3195 (9)	37 (2)
C(4)	−830 (10)	−692 (9)	4046 (8)	30 (2)
C(5)	1962 (11)	−1773 (9)	4766 (8)	34 (2)
C(6)	41 (10)	−2111 (8)	900 (8)	29 (2)
C(7)	−2399 (11)	−1498 (9)	1 (8)	31 (2)
C(8)	−2354 (10)	−1355 (8)	2041 (8)	27 (2)
C(9)	−2700 (10)	558 (8)	234 (8)	29 (2)
C(10)	−5224 (16)	869 (13)	3078 (12)	62 (3)
C(11)	−5659 (15)	2193 (12)	2624 (12)	56 (3)
C(12)	−6096 (17)	2585 (15)	4316 (13)	68 (4)
C(13)	−7632 (18)	3282 (15)	4360 (15)	75 (4)
C(14)	−243 (22)	4471 (18)	1700 (16)	89 (5)
C(15)	−1026 (23)	4841 (21)	2632 (19)	101 (6)
C(16)	−3376 (25)	5531 (22)	3375 (21)	111 (7)
C(17)	−4982 (22)	5588 (19)	3442 (17)	93 (6)
C(18)	−3570 (13)	4982 (11)	−34 (10)	44 (3)
C(19)	−5876 (13)	5237 (12)	908 (11)	50 (3)
O(1)	936 (11)	−3570 (9)	3578 (9)	68 (3)
O(2)	4340 (11)	−1360 (10)	2045 (9)	68 (3)
O(3)	1129 (9)	1559 (7)	3125 (7)	48 (2)
O(4)	−2003 (9)	−443 (7)	4418 (7)	45 (2)
O(5)	2439 (9)	−2445 (8)	5644 (7)	52 (2)
O(6)	1046 (8)	−2945 (7)	1117 (7)	43 (2)
O(7)	−2931 (10)	−1908 (8)	−410 (7)	54 (2)
O(8)	−2837 (8)	1677 (7)	2955 (6)	42 (2)
O(9)	−3510 (8)	1500 (7)	−42 (7)	44 (2)
O(10)	−5330 (9)	2758 (8)	3312 (7)	49 (2)
O(11)	−2504 (11)	4894 (9)	2681 (8)	61 (2)
O(12)	−4439 (7)	4576 (6)	1025 (6)	38 (2)

[a] Equivalent isotropic U defined as one-third of the trace of the orthogonalized U_{ij} tensor.

$(CO)_4$". Instead we obtained a dimer, $[W(CO)_5SnClFe(CO)_4]_2[Na_2((C_2H_5)_2O)_4(C_4H_8O_2)]$ (**1**), whose properties and structure we report here.

Results

Treatment of a tetrahydrofuran solution of $[W(CO)_5SnCl_2(OC_4H_8)]$ with solid $Na_2Fe(CO)_4 \cdot 1.5C_4H_8O_2$ at −78 °C produces an opaque brown solution. Evaporation of solvent followed by redissolution in diethyl ether, filtration, and cooling to −20 °C produces brown crystals of $[W(CO)_5SnClFe(CO)_4]_2[Na_2((C_2H_5)_2O)_4(C_4H_8O_2)]$ (**1**) in 63% yield. Efforts to remove sodium chloride from this cluster including attempted sublimation and dissolution in nonpolar solvents (hexane, toluene) did not produce evidence for the formation of "$(OC)_5WSn{=}Fe(CO)_4$".

The Structure As Determined by X-ray Crystallography. The asymmetric unit contains half of the $[(OC)_5WSnClFe(CO)_4]_2^{2-}$ cluster, a sodium ion, two diethyl ether molecules, and half of a dioxane molecule. Atomic positional parameters are given in Table I. Table II presents selected interatomic distances and angles.

The solid consists of a novel layered array, which we will discuss first in terms of the geometry of a cluster consisting of $[(OC)_5WSnClFe(CO)_4]_2^{2-}$ and the sodium ion coordination and then show how these interact.

The dianion is a centrosymmetric dimer built around a planar Sn_2Fe_2 core. A view of this cluster is given in Figure 1. The tin atoms are four-coordinate with flattened tetrahedral geometry. The $SnFe_2W$ unit is nearly planar with the tin atom only 0.554 (4) Å out of the Fe_2W plane. The sum of the base angles (2 W–Sn–Fe and Fe–Sn–Fe) is 347.7°, closer to the ideal 360° for trigonal-pyramidal geometry than the 328.5° expected for tetrahedral coordination. Since the tin atom is slightly out of the WFe_2 plane, the Cl–Sn–Fe angles (103.0 (1), 101.5 (1)°) and the Cl–Sn–W angle (100.8 (1)°) are somewhat greater than 90°. The

Table II. Selected Interatomic Distances and Angles for **1**[a]

	Interatomic Distances (Å)		
Fe–Sn	2.694 (2)	Fe–C(6)	1.767 (8)
Fe–C(7)	1.793 (14)	Fe–C(,)	1.785 (9)
Fe–C(9)	1.783 (9)	Fe–Sn*	2.681 (1)
W–Sn	2.799 (1)	W–C(1)	1.994 (15)
W–C(2)	2.026 7(11)	W–C(3)	2.019 (13)
W–C(4)	2.027 (9)	W–C(5)	1.942 (11)
Sn–Cl	2.505 (3)	Cl–Na	2.691 (5)
Na–O(10)	2.252 (10)	Na–O(11)	2.366 (14)
Na–O(12)	2.329 (8)	Na–O(5+)	2.350 (10)
	Interatomic Angles (deg)		
Sn–Fe–C(6)	79.7 (4)	Sn–Fe–C(7)	169.6 (3)
C(6)–Fe–C(7)	97.2 (5)	Sn–Fe–C(8)	89.1 (4)
C(6)–Fe–C(8)	95.0 (4)	C(7)–Fe–C(8)	101.0 (5)
Sn–Fe–C(9)	85.4 (4)	C(6)–Fe–C(9)	161.1 (5)
C(7)–Fe–C(9)	95.4 (5)	C(8)–Fe–C(9)	96.2 (4)
Sn–Fe–Sn*	79.7 (1)	C(6)–Fe–Sn*	84.7 (3)
C(7)–Fe–Sn*	90.1 (3)	C(8)–Fe–Sn*	168.8 (4)
C(9)–Fe–Sn*	81.3 (3)	Sn–W–C(1)	90.6 (4)
Sn–W–C(2)	88.2 (3)	C(1)–W–C(2)	95.1 (5)
Sn–W–C(3)	86.1 (3)	C(1)–W–C(3)	174.7 (5)
C(2)–W–C(3)	89.0 (5)	Sn–W–C(4)	87.3 (3)
C(1)–W–C(4)	88.2 (5)	C(2)–W–C(4)	174.4 (4)
C(3)–W–C(4)	87.5 (4)	Sn–W–C(5)	178.2 (3)
C(1)–W–C(5)	90.4 (5)	C(2)–W–C(5)	93.1 (4)
C(3)–W–C(5)	92.7 (5)	C(4)–W–C(5)	91.4 (4)
Fe–Sn–W	122.4 (1)	Fe–Sn–Cl	103.0 (1)
W–Sn–Cl	100.8 (1)	Fe–Sn–Fe*	100.3 (1)
W–Sn–Fe*	125.0 (1)	Cl–Sn–Fe*	101.5 (1)
Sn–Cl–Na	157.8 (1)	Cl–Na–O(10)	104.9 (3)
Cl–Na–O(11)	120.2 (3)	O(10)–Na–O(11)	134.9 (4)
Cl–Na–O(12)	89.2 (2)	O(10)–Na–O(12)	87.7 (3)
O(11)–Na–O(12)	92.7 (3)	Cl–Na–O(5+)	96.9 (3)
O(10)–Na–O(5+)	88.4 (3)	O(11)–Na–O(5+)	86.4 (4)
O(12)–Na–O(5+)	173.4 (3)		

[a] Symmetry code: * = −x, y, −z; + = −x, y, 1 −z.

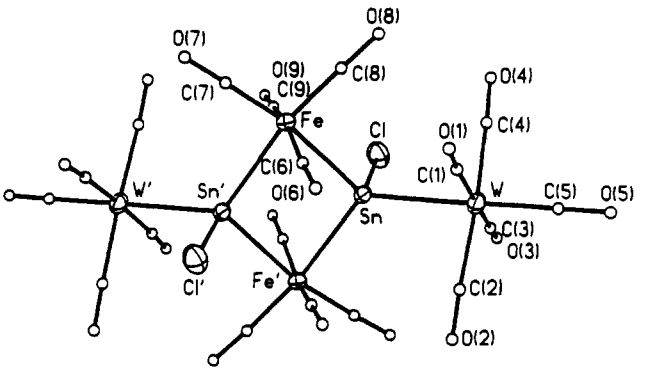

Figure 1. Perspective drawing of $[W(CO)_5SnClFe(CO)_4]_2^{2-}$ showing the atomic numbering scheme.

iron atom has a distorted-octahedral coordination while the tungsten atom has a more regular octahedral geometry.

The structure of the inner core of the cluster dianion is similar to that of two related molecules: $[(CH_3)_2SnFe(CO)_4]_2$ (**2**)[7] and $[(CH_3)_2Sn\{Fe(CO)_4\}_2]_2Sn$ (**3**).[8] All have planar Fe_2Sn_2 rings with

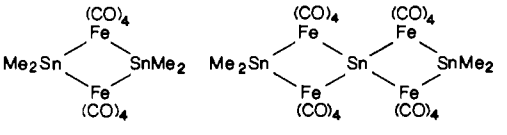

Fe–Sn–Fe angles widened above 90° and Sn–Fe–Sn angles narrowed below 90°. In each case the axial C–Fe–C angles (corresponding to the C(6)–Fe–C(9) angle in **1**) are bent inward

(7) Gilmore, C. J.; Woodward, P. *J. Chem. Soc., Dalton Trans.* **1972**, 1387.
(8) Sweet, R. M.; Fritchie, C. J., Jr.; Schunn, R. A. *Inorg. Chem.* **1967**, *6*, 749.

over the Fe_2Sn_2 ring so that there are relatively close axial contacts between the carbonyl oxygens. In **1** the nonbonded O(6)···O(9)′ contact is 3.29 Å. The Fe–Sn distances (Å) in the Fe_2Sn_2 rings of **1** (2.694 (2)), **2** (2.631 (11)),[7] and **3** (2.735 (10), 2.766 (10), 2.606 (10), 2.623 (10))[8] are quite similar. In both **2** and **3** the Fe_2Sn_2 plane bisects the CH_3–Sn–CH_3 angle. In **1**, however, the tungsten atoms residue much closer to the Fe_2Sn_2 plane than do the chloride ligands, so that the W–Sn–Cl angle is not bisected by the Fe_2Sn_2 plane. This displacement of the $W(CO)_5$ unit nearer the Fe_2Sn_2 plane probably arises from steric affects caused by the bulk of the tungsten substituent. Compound **1** is obtained from a Sn(II) precursor by a halide displacement reaction, while **2** and **3** are obtained by nonredox routes from Sn(IV) compounds. Nevertheless, the bonding within each cluster, **1**, **2** or **3**, must be similar. There are sufficient electrons to have two-electron bonds between each Sn–Fe. Realizing that a $W(CO)_5^{2-}$ group, chloride ion, and a methyl anion are isolobal, one can view all of the clusters **1**, **2**, and **3** as derived from a common core.

The geometry of the $SnW(CO)_5$ portion of the cluster is quite regular. The Sn–W distance (2.799 (1) Å) falls at the long end of the narrow range (2.702–2.794 Å) of previously reported Sn–W distances involving various $SnW(CO)_5$ groups.[2,4,9] The shortening of the W–C(5) bond (1.942 (11) Å) relative to the other W–C bonds (range 1.994 (15)–2.027 (9) Å) is a consequence of its position trans to the tin ligand. This effect is seen in $(OC)_5W$-$SnCl_2(OC_4H_8)$ and $(OC)_5WSnCl_2(OC_4H_8)_2$ as well as other tin/transition-metal complexes.[4]

The Sn–Cl distance (2.505 (3) Å) is exceptionally long. The Sn–Cl distances are much shorter in $(OC)_5WSnCl_2(OC_4H_8)$ (2.352 (3), 2.375 (2) Å) and in $(OC)_5WSnCl_2(OC_4H_8)_2$ (2.371 (2), 2.364 (2) Å).[4] A comparably long Sn–Cl distance of 2.50 (1) Å is found, however, in $[(\eta^5\text{-}C_5H_5)Fe(CO)_2][(\eta^5\text{-}C_5H_5)Mo(CO)_3]SnCl$.[10]

Each sodium ion is coordinated by two diethyl ether molecules, a dioxane molecule, a carbonyl group of the $W(CO)_5$ fragment, and a chloride (from the Cl–Sn unit). The Na–O contacts (Na–O(5), 2.350 (10); Na–O(10), 2.352 (10); Na–O(11), 2.366 (14); Na–O(12), 2.329 (8) Å) fall into a narrow range. The proximity of the sodium ion to a carbon monoxide ligand is not unusual. Similar contacts are found, for example, in the salt $Na_2Fe(CO)_4 \cdot 1.5C_4H_8O_2$.[11] The Na–Cl contact (2.691 (5) Å) is shorter than that observed in sodium chloride (2.81 Å).[12] Notice that this short Na–Cl distance is correlated with a long Sn–Cl distance. The coordination of the sodium ion is roughly trigonal bipyramidal with the NaClO(10)O(11) unit nearly planar.

The formation of a layer through the interrelationship of these two structural elements, the cluster and the sodium ion environments, is best seen by turning to Figure 2. In this figure, all of the carbonyl groups of the clusters have been omitted except for the ones that bridge W and Na. As can be seen, a complex network exists in which each cluster is connected to two adjacent sodium ions through chloride bridges. Each sodium ion makes contact with another cluster through a carbonyl group. Finally, each sodium ion is connected to another sodium ion through a bridging dioxane molecule. Within this layer, there are four distinct centers of symmetry. One is located at the center of a Fe_2Sn_2 group. Another is located at the middle of a dioxane molecule. The third is located within the $(ClSnWCONa)_2$ ring, and a fourth is located at the midpoint of the line joining W⁺ and W″. The interrelationship between the layers is best seen in Figure 3. All contacts between individual layers are of normal van der Waals type.

Spectroscopic Measurements. The infrared spectrum of a tetrahydrofuran solution of **1** shows seven absorbances in the carbonyl region: 2068 (w), 2045 (m), 2025 (m), 1998 (m), 1987 (s), 1921 (s), 1897 (s) cm^{-1}. The number of carbonyl stretching

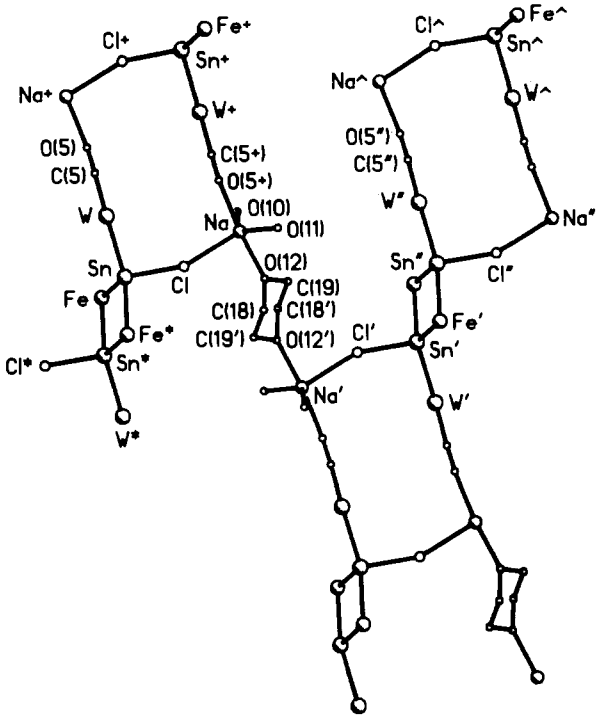

Figure 2. View of one layer of **1** with all carbon monoxide ligands, except for the one closest to the sodium ions, and the ethyl groups omitted.

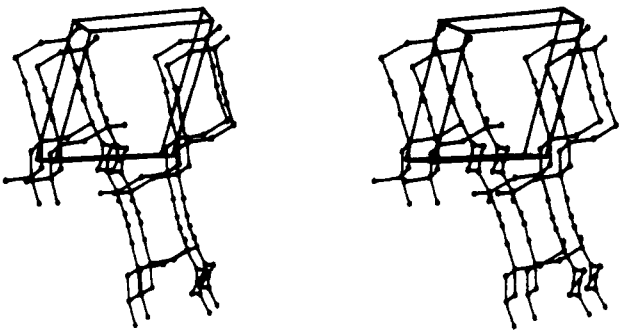

Figure 3. Stereoscopic view illustrating the relationship of two layers (which are drawn with carbonyl and ethyl groups omitted as in Figure 2).

frequencies and their positions are consistent with the sum of those found in the $W(CO)_5L$ compounds $W(CO)_5SnCl_2(OC_4H_8)_n$ (n = 1, 2)[4] and the $Fe(CO)_4L_2$ compounds $[R_2SnFe(CO)_4]_2$ (R = CH_3, C_6H_5, t-C_4H_9).[13]

The ^{119}Sn NMR spectrum of the dianion in tetrahydrofuran solution consists of a single peak at 453 ppm. No satellites due to coupling to tungsten could be observed. The chemical shifts of Sn(II) in polynuclear compounds are strongly dependent on the identity of the transition metal to which they are bound.[14] For example, $[(CO)_5CrSnCl_2(OC_4H_8)]$[15] has a chemical shift of 193 ppm and $[(CO)_5WSnCl_2(OC_4H_8)]$[15] has a chemical shift of −54.6 ppm. The chemical shift of a compound similar to the dianion is not available for comparison.

Experimental Section

Materials. The $Na_2Fe(CO)_4 \cdot 1.5C_4H_8O_2$ was purchased from Alfa Products and used without further purification, and $[W(CO)_5SnCl_2(O$-$C_4H_8)]$ was prepared as described previously.[4] Solvents were carefully dried and purged of oxygen before use. All reagents and products were handled with the exclusion of air by standard Schlenk techniques.

Physical Measurements. The ^{119}Sn NMR spectra were recorded on a Nicolet NT-200 Fourier transform spectrometer operating at 74.5 MHz using quadrature detection. The spectra were obtained with 12-

(9) Scheidsteger, O.; Huttner, G.; Dehnicke, K.; Pebler, S. *Angew. Chem., Int. Ed. Engl.* **1985**, *24*, 428.
(10) O'Connor, J. E.; Corey, E. R. *J. Am. Chem. Soc.* **1967**, *89*, 3930.
(11) Chin, H. B.; Bau, R. *J. Am. Chem. Soc.* **1976**, *98*, 2434.
(12) Pauling, L. *The Nature of the Chemical Bond*, 3rd ed.; Cornell University Press: Ithaca, NY, 1960; p 520.
(13) Marks, T. J.; Newman, A. R. *J. Am. Chem. Soc.* **1973**, *95*, 769.
(14) Petz, W. *Chem. Rev.* **1986**, *86*, 1019.
(15) du Mont, W. W.; Kroth, H. J. *Z. Naturforsch.* **1980**, *35B*, 700.

Table III. Crystallographic Data for $[W(CO)_5SnClFe(CO)_4]_2[Na_2((C_2H_5)_2O)_4(C_4H_8O_2)]$ (**1**) at 130 K

chem formula	$C_{38}H_{48}Cl_2Fe_2Na_2O_{24}Sn_2W_2$
fw	1722.46
space group	$P\bar{1}$ (No. 2)
a, Å	9.919 (2)
b, Å	12.656 (3)
c, Å	13.131 (4)
α, deg	67.72 (2)
β, deg	77.65 (4)
γ, deg	70.67 (2)
V, Å^3	1432.0 (6)
D(calcd, 130 K), g/cm^3	1.38
Z	1
radiation; λ, Å	Mo Kα; 0.71069
μ(Mo Kα) cm^{-1}	57.67
transmission factors	0.36-0.68
$R(F_o)$	0.057
$R_w(F_o)$	0.063

mm tubes and broad-band proton decoupling. An external $Sn(CH_3)_4$ reference and the high frequency positive convention were used in reporting all chemical shifts. Infrared spectra were recorded in tetrahydrofuran solution on an IBM IR32 Fourier transform infrared spectrometer.

Synthesis of $[W(CO)_5SnClFe(CO)_4]_2[Na_2((C_2H_5)_2O)_4(C_4H_8O_2)]$ (1). Solid $Na_2Fe(CO)_4 \cdot 1.5C_4H_8O_2$ (1.24 g, 3.58 mmol) was added slowly to $[W(CO)_5SnCl_2(OC_4H_8)]$ (2.10 g, 3.58 mmol) in 30 mL of tetrahydrofuran at -78 °C. The reaction mixture progressively turned dark brown during the addition. The reaction mixture was allowed to come to room temperature and then stirred for an additional 1 h. At this point everything had dissolved to form a dark brown, opaque solution. The tetrahydrofuran was removed under vacuum, and the brown residue was redissolved in 40 mL of diethyl ether. Filtration of this solution through a bed of Celite and concentration to about 25 mL followed by slow cooling to -20 °C gave 1.22 g of brown crystals in 63% yield.

X-ray Data Collection. Brown plates were formed by slowly cooling (from +23 to -20 °C) a saturated diethyl ether solution of the compound. The crystals were removed from the Schlenk tube under a stream of dry nitrogen and quickly covered with a light hydrocarbon oil (Exxon Paratone N) to protect them from the atmosphere. The crystal was mounted on a glass fiber and secured in the nitrogen cold stream of a $P2_1$ diffractometer equipped with a locally modified LT-1 low-temperature apparatus and a graphite monochromator. Data were collected at 130 K. Unit cell parameters were obtained from a least-squares refinement of 10 reflections with $17 < 2\theta < 26°$. The crystal lattice was found to be triclinic P by the automatic indexing routine of the software available on the diffractometer; no symmetry was observed in any of the axial photographs. A unique hemisphere of data was collected to a $2\theta_{max}$ of 50 °C, yielding 5531 data. A total of 4514 data with $I > 3\sigma(I)$ were used in the solution and refinement of the structure. No decay in the intensities of two standard reflections occurred. Crystal parameters are summarized in Table III. The data were corrected for Lorentz and polarizaion effects.

Solution and Refinement of Structure. The positions of tin, tungsten, and iron were generated by FMAP 8, the Patterson-solving routine of SHELXTL, version 5. Other atom positions were located from successive difference Fourier maps. Anisotropic thermal parameters were assigned to the tin, tungsten, iron, sodium, and chlorine atoms. Isotropic thermal parameters were used for the remaining atoms. Hydrogen atoms were placed at idealized positions (d(C-H) = 0.96 Å) and assigned isotropic thermal parameters 20% greater than the carbon atom to which they were attached. They were refined by using a riding model. A correction for absorption was applied.[16] Neutral-atom scattering factors were those of Cromer and Waber.[17] The largest feature on the final difference Fourier map was 2.8 e/Å^3. This peak was 1.01 Å from the tungsten atom.

Acknowledgment. We thank the National Science Foundation (Grant CHE-8519557) for support.

Registry No. 1, 116887-72-0; $[W(CO)_5SnCl_2(OC_4H_8)]$, 65198-59-6; $Na_2Fe(CO)_4 \cdot 1.5C_4H_8O_2$, 59733-73-2; Fe, 7439-89-6; Sn, 7440-31-5; W, 7440-33-7.

(16) XABS produces an absorption tensor from an expression relating F_o and F_c: Moezzi, B. Ph.D. Thesis University of California, Davis, CA, 1988.

(17) *International Tables for X-ray Crystallography*; Kynoch: Birmingham, England, 1974; Vol. 14, pp 149-150, 99-101.

Supplementary Material Available: Listings of all bond lengths, bond angles, hydrogen atom positions, anisotropic thermal parameters, and data collection parameters and three views of structural elements (8 pages); a listing of observed and calculated structure factors (27 pages). Ordering information is given on any current masthead page.

Contribution from the Institute of Inorganic and Applied Chemistry, University of Hamburg, D-2000 Hamburg 13, FRG

Interaction of Vanadate ($H_2VO_4^-$) with Dipeptides Investigated by ^{51}V NMR Spectroscopy

Dieter Rehder

Received February 24, 1988

Vanadium is rapidly attaining the status of a widely spread biometal in both its oxidation states V (where it is present, at physiological pH, in the form of dihydrogen orthovanadate and several condensated species[1]) and IV/III. Two enzymes containing vanadium as an essential metal have been discovered recently: (i) a vanadate(V)-dependent haloperoxidase present in marine brown and red algae[2,3] and in a lichen[4] and (ii) nitrogenases isolated from specific strains of *Azotobacter vinelandii* and *Azotobacter chroococuum*, which contain vanadium instead of molybdenum.[5] The importance of vanadium in nitrogen fixation has in fact been documented already more than a half-century ago.[6] Further, the chemical similarity between inorganic phosphate and vanadate has prompted a number of investigations into the possible antagonism between these two anions in bioreactions[7] ever since the discovery of the inhibitory action of vanadate toward the sodium-potassium pump.[8] Both inhibitory and stimulating functions of vanadate have been documented,[9] which makes this anion also interesting in medication and in toxicological studies. In most if not all of its actions, vanadate is or becomes an integral part of a large protein molecule. Despite a few investigations concerned with the coordination of V(V), V(IV), and V(III) to serum transferrin[10,11] and the interaction of vanadate(V) with ribo-

(1) (a) Pettersson, L.; Hedman, B.; Andersson, I.; Ingri, N. *Chem. Scr.* **1983**, *22*, 254. (b) Pettersson, L.; Andersson, I.; Hedman, B. *Chem. Scr.* **1985**, *25*, 309. (c) Pettersson, L.; Hedman, B.; Nenner, A.-M; Andersson, I. *Acta Chem. Scand., Ser. A* **1985**, *A39*, 499. (d) Ivakin, A. A.; Kurbatova, L. D.; Kruchinina, M. V.; Medvedeva, N. I. *Russ. J. Inorg. Chem.* (*Engl. Transl.*) **1986**, *31*, 219. In this communication, a trinuclear species, $V_3O_{10}^{5-}$, and its monoprotonated form are described in addition to the vanadates reported by Pettersson et al.

(2) (a) Vilter, H. *Phytochemistry* **1984**, *23*, 1387. (b) de Boer, E.; van Kooyk, Y.; Tromp, M. G. M.; Plat, H.; Wever, R. *Biochim. Biophys. Acta* **1986**, *869*, 48.

(3) Krenn, B. E.; Plat, H.; Wever, R. *Biochim. Biophys. Acta* **1987**, *912*, 287.

(4) Plat, H.; Krenn, B. E.; Wever, R. *Biochem. J.* **1987**, *248*, 277.

(5) (a) Robson, R. L.; Eady, R. R.; Richardson, T. H.; Miller, R. W.; Hawkins, M.; Postgate, J. R. *Nature* (*London*) **1986**, *322*, 388. (b) Arber, M. J.; Dobson, B. R.; Eady, R. R.; Stevens, P.; Hasnain, S. S.; Garner, C. D.; Smith, B. E. *Nature* (*London*) **1987**, *325*, 372.

(6) Bortels, H. *Zentralbl. Bakteriol.* **1936/37**, *95*, 13.

(7) Gresser, M. J.; Tracey, A. S.; Stankiewicz, P. J. *Adv. Protein Phosphatases* **1987**, *4*, 35.

(8) Cantley, L. D., Jr.; Josephson, L.; Warner, R.; Yanagisawa, M.; Lechene, C.; Guidotti, G. *J. Biol. Chem.* **1977**, *252*, 7421.

(9) For a comprehensive account see: Chasteen, N. D. *Struct. Bonding* (*Berlin*) **1983**, *53*, 105.

(10) Butler, A.; Danzitz, M. J. *J. Am. Chem. Soc.* **1987**, *109*, 1864. There are arguments against the assignment of the signals observed at -530 ppm to transferrin-bound vanadate: In a large molecule containing a quadrupolar nucleus, the long molecular correlation time should give rise to signals of at least several kilohertz in width. We feel that the rather sharp signals described in this communication are due to complex formation of vanadate with small fragments of transferrin.

(11) (a) Chasteen, N. D.; Grady, J. K.; Holloway, C. E. *Inorg. Chem.* **1986**, *25*, 2754. (b) Bertini, I.; Canti, G.; Luchinat, C. *Inorg. Chim. Acta* **1982**, *67*, L21.

0020-1669/88/1327-4312$01.50/0